Clays and Clay Minerals, Vol. 37, No. 1, 1–11, 1989.

HIGH-RESOLUTION TRANSMISSION ELECTRON MICROSCOPY OF MIXED-LAYER ILLITE/SMECTITE: COMPUTER SIMULATIONS

GEORGE D. GUTHRIE, JR. AND DAVID R. VEBLEN

Department of Earth and Planetary Sciences
The Johns Hopkins University, Baltimore, Maryland 21218

Abstract—High-resolution transmission electron microscope images of dioctahedral mixed-layer clay structures (illite/smectite) having various substitutional and polytypic schemes were modeled using computer simulation methods. Both one- and two-dimensional calculations were performed using parameters characteristic of a typical range of imaging conditions. One-dimensional images formed by imaging only 00*l* diffractions show three important results: (1) The 20-Å periodicity resulting from rigorously ordered R1 illite/smectite can be imaged, but unconventional focus conditions may be necessary. (2) For crystals oriented with the electron beam perfectly parallel to the layers, the brightest fringes in the image correspond to either the octahedral sheets or the interlayer sites, depending on focus conditions. Misorientation of the crystal, however, by only 1° or 2° shifts the positions of the fringes by 1 to 3 Å. Furthermore, in tilted specimens, some defocus values produce images suggesting that smectite layers have a 11–13-Å periodicity, despite the uniform 10-Å periodicity present in the model structure. Thus, direct correlations between image and structure generally should not be made. (3) Two-layer polytypes of pure illite or pure smectite can also produce images with a 20-Å periodicity.

Two-dimensional images additionally showed that the cross fringes produced by some *hkl* diffractions can be imaged. The simulations showed that these cross fringes ideally might permit the determination of both layer stacking and compositional periodicity, but the fringes are lost by misorientations of a few degrees. These image simulations demonstrated, therefore, that mixed layering of illite and smectite theoretically can be directly imaged by transmission electron microscopy of chemically untreated specimens, but ambiguities may exist in the detailed intepretation of the images.

Key Words—High-resolution transmission electron microscopy, Illite, Image simulation, Mixed layer, Smectite.

INTRODUCTION

High-resolution transmission electron microscopy (HRTEM) is a powerful tool for the study of imperfectly crystalline materials. HRTEM experiments that involve the direct imaging of the crystal structure or lattice periodicity have been applied successfully to numerous problems in the crystal chemistry of rock-forming silicates (for reviews, see Spence, 1981; Veblen, 1985a, 1985b, 1989). The HRTEM technique also holds great promise for elucidating the microstructures of clay minerals, despite inherent problems with specimen preparation and damage in the relatively intense electron beam necessary for HRTEM work. Perhaps the most promising application in clay mineralogy is the potential for imaging sequences of different layer types in mixed-layer clays; in fact, HRTEM already has been used to determine the structures of defects based on mixed-layering disorder in macrocrystalline igneous and metamorphic chlorites and micas (see above references for examples).

A number of reports have recently appeared involving the application of HRTEM methods to illite/smectite (I/S) mixed-layer clays and rectorites (McKee and Buseck, 1978; Ahn and Peacor, 1985, 1986a, 1986b; Klimentidis and Mackinnon, 1986; Bell, 1986; Lee *et al.*, 1985, 1986; Hansen and Lindgreen, 1987). Unfortunately, experimental techniques and, even more so, the interpretation of HRTEM images from I/S have been highly non-uniform from investigator to investigator. To date, all published interpretations of HRTEM data from I/S have been purely intuitive, despite the fact that reliable image interpretation generally requires computer simulation of dynamical diffraction effects and electron optical parameters. Because of the importance of these HRTEM studies on I/S, we initiated the present study to provide a solid theoretical basis for future investigations.

Iijima and Buseck (1978) simulated images of a $2M_1$ muscovite to show that polytypism can be detected in two-dimensional *a*-axis HRTEM images. Amouric *et al.* (1981) also simulated two-dimensional images for $1M$ phlogopite and $1M$, $2M_1$ and $3T$ muscovite. They showed that under very restrictive experimental conditions, contrast details in HRTEM images of these minerals reflect variations in the charge density of the structure. Under optimum experimental conditions, however, images can give incorrect information about the structure (i.e., false stacking sequences and false thicknesses for individual layers).

Computer simulations are particularly important for interpreting images of I/S, in which the major structural building blocks are all essentially identical (i.e., 2:1 layers) and the differences being imaged are relatively subtle. In fact, under the high-vacuum conditions in the TEM, smectite can lose its interlayer water

Copyright © 1989, The Clay Minerals Society

https://doi.org/10.1346/CCMN.1989.0370101 Published online by Cambridge University Press

and collapse (see, e.g., Klimentidis and Mackinnon, 1986; Ahn and Peacor, 1986a); if this occurs, the major difference between layers is compositional. Attempts to amplify the difference between layers by expanding the smectite interlayers with suitable polymers have yielded widely different results. We have restricted our study to I/S that is chemically untreated and collapsed to a uniform 10-Å spacing between the octahedral sheets of all adjacent 2:1 layers.

Within this framework, the following questions were posed that could be addressed by modern methods of computer simulation:

(1) For a model I/S structure, can periodicities due to ordering of illite and smectite layers be imaged in electron microscopes of moderate resolution that are commonly accessible to mineralogists?
(2) If the I/S ordering can be imaged, what are the best electron optical conditions for such experiments?
(3) What is the correspondence between I/S images and the actual structure under various imaging conditions, or, posed in a different fashion, do the fringes in images of I/S really correspond to the positions of the layers in the structure?
(4) Finally, can image characteristics due to other structural phenomena, such as polytypism, be confused with those resulting from I/S mixed layering?

As an extension of this study, we have applied the results of our computer simulations to experimental HRTEM images from an R1 I/S and an R3 I/S that had been characterized by X-ray powder diffraction methods as very well-ordered. We will report these experimental results in a separate publication.

HRTEM IMAGE SIMULATIONS

General background

Although the computer simulation of HRTEM images is now standard practice in fields routinely employing high-resolution microscopy (e.g., solid-state chemistry, physics, materials science), it is probably unfamiliar to many clay mineralogists. The procedure is therefore briefly summarized here. Reviews of HRTEM image simulation were given by O'Keefe *et al.* (1978), O'Keefe (1984), and Self and O'Keefe (1988); Veblen (1985a) presented a brief review intended for earth scientists.

The need for image simulations arises because it is generally not possible to work backwards from a HRTEM image to reconstruct a unique structure for the imaged crystal. It is, however, possible to calculate the HRTEM images that should arise from a given model structure if it is imaged with various electron optical conditions. If the microscopist can obtain good matches between images computed from a structural model and those obtained experimentally, the model probably is correct. Another important use of image simulations is to help answer questions about the imaging of specific structures. This approach is used here to answer questions such as those posed in the Introduction.

The first step in the simulation of a HRTEM image is to calculate the diffracted electron wave field that emerges from the bottom of the thin crystalline specimen. Because the interaction of electrons with matter is far stronger than that for X-rays, the scattering is strongly dynamical, even for very thin crystals (i.e., multiple scattering of electrons must be taken into account in the calculation). This dynamical diffraction calculation is generally performed using the "multislice" approach (Cowley and Moodie, 1957), in which the crystal is divided into a series of thin slices; the diffracted phases and amplitudes are calculated iteratively by adding on more and more slices to build up the desired crystal thickness. Effects on the image from slight misorientation can be evaluated by performing the dynamical diffraction calculation for crystals that are tilted slightly out of perfect zone-axis orientation in various directions.

Following the diffraction calculation, the effects of the electron microscope optics on the diffracted phases and amplitudes are considered. These effects include phase shifts of the diffracted beams due to the spherical aberration of the objective lens and the microscope defocus; changes in phase and amplitude due to chromatic aberration; elimination of image contributions from diffracted beams that fall outside the objective aperture; smearing effects due to a convergent, rather than parallel, electron beam and physical vibrations; possible effects due to various types of misalignment of the microscope; and contrast variations resulting from film exposure characteristics and photographic printing procedures.

After a series of images has been calculated, hard copies typically are produced with an output device that is capable of halftone reproduction (such as a line printer run in overprint mode). Images are usually simulated for a range of crystal thicknesses, microscope defocus values, and perhaps crystal orientations. Finally, the simulated and experimental images are compared visually.

Simulation procedures and model structures

HRTEM image simulations for the present study were performed with the SHRLI set of computer programs, version 80F (O'Keefe, 1984). The calculations were carried out with a MicroVAX-II computer, and images were printed with a dot-matrix lineprinter using an output routine originally written by Peter G. Self, University of Melbourne, Melbourne, Australia, and subsequently modified by Judith Konnert, U.S. Geological Survey, Reston, Virginia.

Inasmuch as no published three-dimensional X-ray crystal structure refinements exist for mixed-layer I/S,

https://doi.org/10.1346/CCMN.1989.0370101 Published online by Cambridge University Press

Table 1. Simulation parameters describing the Philips 420 and JEOL 100C electron microscopes.

	Imaging conditions	
	Philips 420	JEOL 100C
kV (keV)	120	100
ΔE (ev)	0.50	0.50
r_{min} (Å)	3.4	5.3
r_{min} (Å^{-1})	0.294	0.1887
C_s (mm)[2]	2.0	8.2
C_c (mm)[3]	2.0	3.9
Del (Å)[4]	150	214
Scherzer defocus (Å)[5]	−1002	−2133

[1] Parameters are theoretical values given by the manufacturers.
[2] Spherical aberration coefficient.
[3] Chromatic aberration coefficient.
[4] Parameter used to describe effect of chromatic aberration.
[5] Theoretical optimum deviation from Gaussian focus.

input structures were derived from the dioctahedral mica structure reported by Richardson and Richardson (1982). The derived structures presumably differ somewhat from real I/S structures; however, they can be used to answer questions about how illite-like and smectite-like site occupancies will perturb images, compared with those from ideal 2:1 layer silicates with, for example, full occupancy of the interlayer sites. Atomic positions for the input models were obtained from a single layer of the $2M_1$ mica (space group $C2/c$) transformed to a $1M$ unit cell (space group $C2/m$; see Appendix I for details of this transformation). The one-layer polytype was chosen so that effects on the images of cation and vacancy substitutions could be isolated from those resulting from polytypism. Following calculation of the atomic coordinates, structures having R1 (. . . ISIS . . .) and R3 (. . . ISIIISII . . .) ordering schemes were built, assuming a 10-Å basal spacing for both I and S layers. Compositions and occupancies were assumed which gave layer charges for illite and smectite of 0.75 and 0.20 per formula unit, respectively. Layer charges were created using the tetrahedral substitution

$$^{IV}Al^{3+} \rightarrow {}^{IV}Si^{4+},$$

which was compensated by the interlayer substitution

$$A_{K^+} \rightarrow A_{\square},$$

in which □ represents a vacancy. The calculations were made with K as the interlayer cation in order to maximize the average atomic number difference and, hence, the contrast between the illite and smectite interlayers. Substitution by lighter cations, such as Na, would cause the same types of changes in image character, but with lesser contrast. Other factors that contribute to contrast (such as the presence of water or other polar molecules in the interlayer site) were not considered in these calculations.

Simulated HRTEM images were computed for a range of imaging conditions, specimen thicknesses, and specimen misorientations. Images were produced for two sets of optical constants (spherical and chromatic aberration coefficients) appropriate for two different microscopes (Philips 420 and JEOL 100C; see Table 1). Defocus, Δf, was varied by ±2000 Å around the Scherzer (optimum) defocus, in steps of 500 Å, and specimen thickness was varied from 52 to 156 Å. Objective aperture size was chosen to correspond to the Scherzer limit; i.e., diffracted beams corresponding to spatial frequencies smaller than the point-to-point resolution of the microscope were excluded from the image.

As noted in the Introduction, experimental imaging of I/S is much more difficult than imaging of most rock-forming minerals, due to very rapid structural damage in the electron beam and small crystal size. These factors combine to prevent the microscopist from accurately orienting the sample, and the beam damage further acts to reduce resolution by forming noncrystalline material on the specimen. As a result, only the basal fringes that are formed by imaging the $00l$ diffracted beams are usually observed, although occasionally cross-fringes with spacing 2.5 Å can be seen.

To simulate these misorientation and damage effects, not only were two-dimensional images formed from $0kl$ diffracted beams calculated, but extensive calculations of one-dimensional images showing only the basal fringes were also made. These calculations were made by removing diffracted beams that did not satisfy the condition $h = k = 0$ prior to running the imaging program of the SHRLI package. In addition, numerous simulations were performed with the crystal tilted slightly out of orientation with respect to the electron beam. These simulations were made by shifting the Laue circle to reciprocal space positions along the $00l$ row during the multislice dynamical diffraction calculation; for the perfect orientations simulations, the Laue circle is centered on the reciprocal space origin. Thus, the simulated misorientations corresponded to small rotations of the crystal about an axis parallel to the layers of the structure and lying in the plane of the thin specimen. No attempt was made to simulate the possible effects of slight rotations around c^*.

SIMULATION RESULTS

As noted above, the calculations simulated the effects on HRTEM images of variations in ordering scheme (R1 and R3) and hence composition, crystal orientation and thickness, and TEM operating conditions and optical constants. Both two-dimensional images and one-dimensional images with basal fringes only were calculated. Except where noted, the calculations refer to conditions in a Philips 420 microscope (Scherzer or point-to-point resolution r_{min} = 3.4 Å). The images presented here are best viewed at low angles parallel to the layers.

https://doi.org/10.1346/CCMN.1989.0370101 Published online by Cambridge University Press

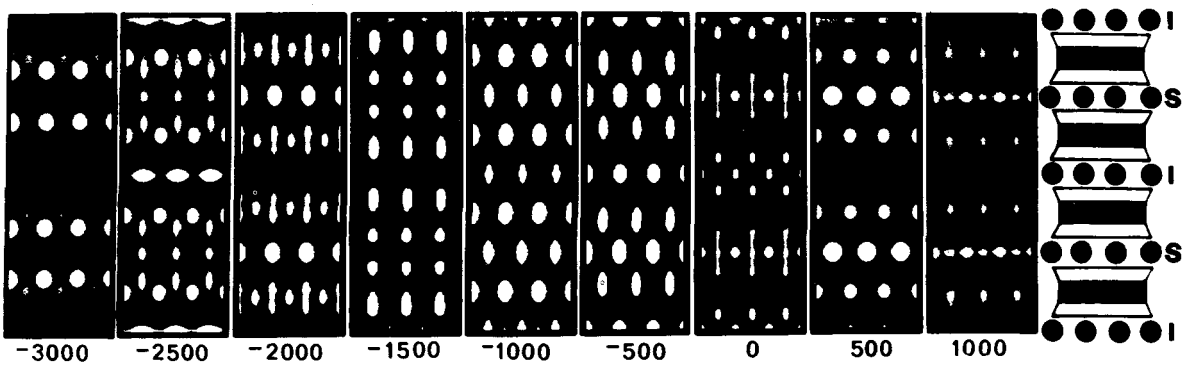


Figure 1. Two-dimensional simulations of R1-ordered illite/smectite for a Philips 420 instrument. Structure was oriented such that the *b*-axis was horizontal and the *c*-axis was vertical; crystal thickness was 156 Å. Defocus (Δf) is given in Å below each simulation; theoretical optimum defocus value (commonly referred to as the Scherzer focus) corresponds roughly to the central simulation, Δf = −1000 Å. Structure at right shows positions partially-occupied potassium sites and 2:1 layers. The interlayer spacing was exactly 10 Å.

Two-dimensional images

Simulations of *a*-axis images of perfectly ordered R1 and R3 I/S showed the familiar 10-Å layer subperiodicity, as well as 4.5-Å cross-fringe periodicity; however, the image details were highly sensitive to changes in defocus. For some focus values, the 20-Å basal periodicity resulting from the R1 ordering was clear (Figure 1, Δf = −3000 Å), but for others it was less obvious, and microscopists might observe only an apparent 10-Å repeat (Figure 1, Δf = −1000 Å). Similarly, R3 ordering produced a clear 40-Å periodicity at some defocus values but not at others.

Images showing the fine detail seen in these simulations have not yet been obtained experimentally; however, these calculations show that if beam damage can be eliminated, perhaps by using a cryogenic stage in a high-voltage microscope, I/S ordering might be observed clearly in two-dimensional HRTEM images.

One-dimensional images

Perfect orientation. One-dimensional simulations of R1-ordered I/S in perfect orientation showed dark fringes with apparent 10-Å periodicity at some focus values (e.g., Figure 2, Δf = −2500 Å, +500 Å). At some other focuses, these broad fringes split into finer fringes that revealed details of both the 10-Å subcell periodicity and the 20-Å true periodicity characteristic of R1 ordering (e.g., Figure 2, Δf = −1000 Å). Simulated images from R3 I/S showed similar variations, but with 40-Å periodicity (Figure 3); however, these types of fine-fringe images seldom, if ever, can be observed experimentally for I/S, probably because the crystals almost invariably deviate at least slightly from perfect orientation and are damaged quickly by the electron beam.

Imperfect orientation. Image simulations for crystals that were tilted so that their layers were not perfectly

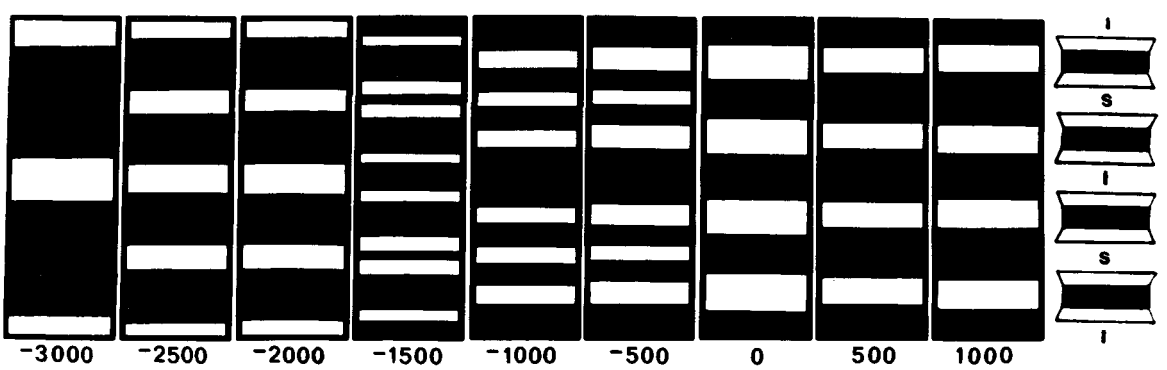


Figure 2. One-dimensional simulations of R1-ordered illite/smectite for a Philips 420 instrument. Simulations assumed the structure to be perfectly oriented, with layers parallel to the central beam. Scherzer focus is shown in the central image. Crystal thickness was 156 Å.

https://doi.org/10.1346/CCMN.1989.0370101 Published online by Cambridge University Press

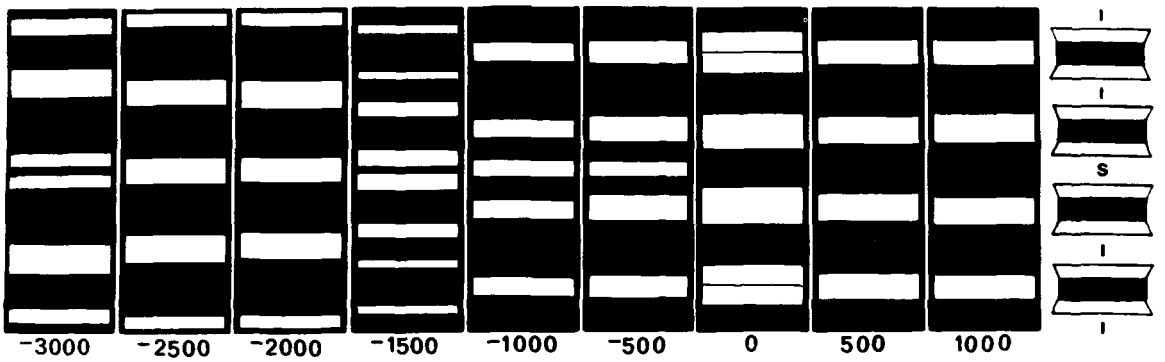


Figure 3. One-dimensional simulations of R3-ordered illite/smectite for a Philips 420 instrument. Simulations assumed perfect orientation. Scherzer focus is shown in the central image. Crystal thickness was 156 Å.

parallel to the electron beam did exhibit the simple dark fringes characteristic of most published I/S images. Examples of such images are shown in Figure 4 for R1 ordering and in Figure 5 for R3 ordering. Even very slight misorientations destroyed the fine image detail seen in simulations from perfectly oriented crystals (Figures 2 and 3).

The tilted-crystal simulations clearly showed an important factor for the experimental imaging of I/S: at the underfocus imaging conditions (negative values of Δf) that are typically used for HRTEM imaging, image superperiodicities due to the ordering were not observed or were very weak (Figure 4, $\Delta f = -1500$ Å, -1000 Å, -500 Å; Figure 5, $\Delta f = -1500$ Å, -1000 Å, -500 Å). In other words, if microscopists were to focus the TEM in the standard way, images of R1 and R3 I/S would show an apparent 10-Å periodicity, with no indication of ordering. However, if the microscope were *overfocused* (e.g., $\Delta f = +500$ to $+1000$ Å), the periodicity due to I/S ordering would become readily apparent. In these images a wide dark fringe was noted close to the smectite interlayers, and narrower dark fringes were noted close to the illite interlayers. This ability to image I/S periodicities in strongly overfocused images was actually observed experimentally first (to be published); the simulations presented here subsequently confirmed that the observed image characteristics were due to I/S ordering.

Effect of crystal thickness. Image simulations have also been used to demonstrate other factors important for imaging of ordering in I/S. Figure 6 shows simulations for R1 crystals of two different thicknesses. Because the intensities of the electron beams carrying information on the I/S ordering were kinematically very low, image periodicities due to the ordering were not apparent in images of thin crystals (e.g., Figure 6, 52 Å thick); however, in thick specimens where the intensities of these beams had been increased through dynamical diffraction, the corresponding image periodicities were readily observed (e.g., Figure 6, 156 Å thick). thick).

Correspondence between image and crystal. Another important point is illustrated by comparing simulations for slightly tilted crystals and perfectly oriented crystals, as shown in Figure 7. Misorientation of the crystal by only a few degrees caused the fringes to shift several Ångstrom units relative to the structure. For

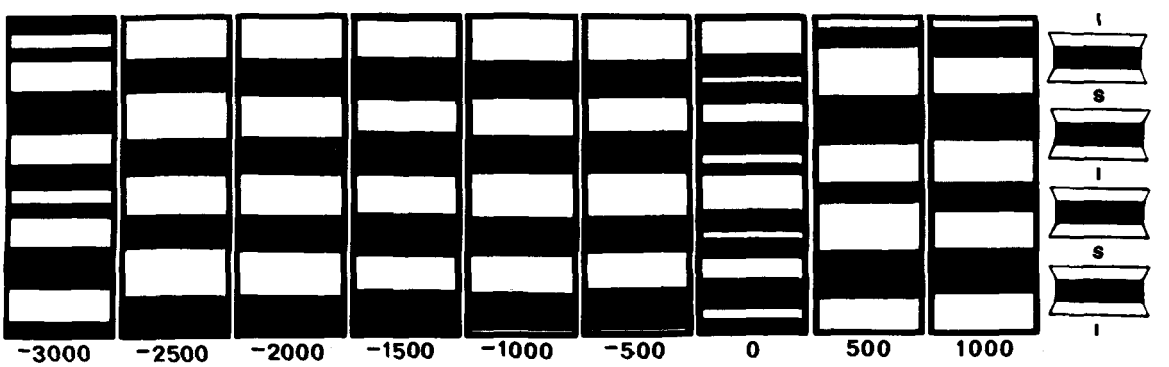


Figure 4. One-dimensional simulations of R1-ordered illite/smectite for a Philips 420 instrument. Simulations assumed that the structure was tilted such that the angle between the central beam and the layers was 3°. Scherzer focus is shown in the central image. Crystal thickness was 156 Å.

https://doi.org/10.1346/CCMN.1989.0370101 Published online by Cambridge University Press

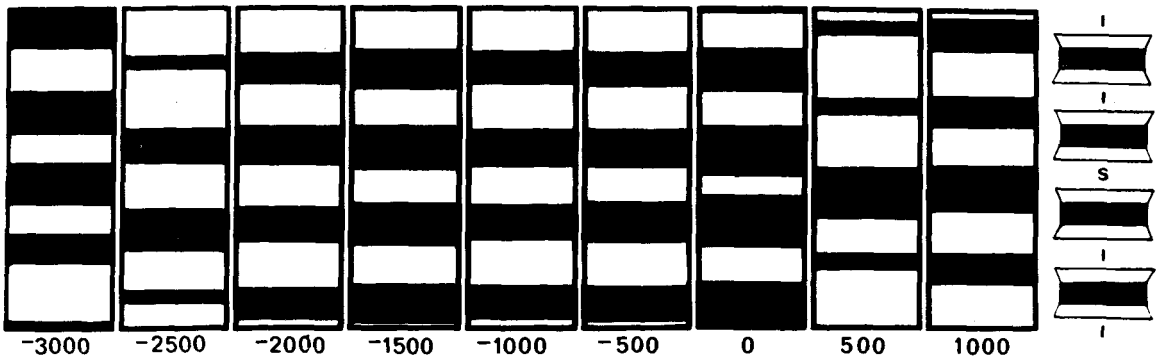


Figure 5. One-dimensional simulations of R3-ordered illite/smectite for a Philips 420 instrument. Simulations assumed the structure to be tilted 3°. Scherzer focus is shown in the central image. Crystal thickness was 156 Å.

the underfocused case (Figure 4, $\Delta f = -1000$ Å), the dark fringes were displaced appreciably from the actual positions of the 2:1 layers of the crystal. Thus, even for underfocus conditions, the fringe positions did not necessarily correspond to layer or atom positions in the crystal structure. For overfocus conditions (Figure 4, $\Delta f = +500$ Å), the dark fringes were near the interlayer positions, rather than near the 2:1 layers, and the fringes for tilted crystals were also shifted relative to the actual structure. The degree of this shift varied with the degree of crystal tilt away from "perfect" orientation (electron beam parallel to the layers). These simulations emphasize that HRTEM images from I/S should not be interpreted too literally, as the exact orientation of a specific region in these fine-grained materials is generally not known. Fringe images should not be interpreted as specific layers in the structure; however, as seen above, the periodicities shown by the fringes may reveal the periodicities in the real crystal, and certain recognizable types of fringes may lie *near* specific structural features.

Apparent layer thicknesses. Although all of the simulations presented in this paper are for structures having 2:1 layers of equal thickness, many of the images showed fringes of more than one width. This is not surprising, because it has been shown both experimentally (Veblen, 1983) and with image simulations (Spinnler *et al.*, 1984) that the apparent thicknesses of the hydroxide and 2:1 layers of chlorite vary with electron optical conditions. Even in perfectly oriented images of chlorite, for example, the fringe corresponding to the hydroxide layer commonly is wider than the thickness of the actual layer, and the width of the 2:1 layer fringe is narrower than the real layer; these thicknesses vary with microscope defocus and other parameters. Amouric *et al.* (1981) found that incorrect thicknesses could be produced for individual layers in two-dimensional images of $2M_1$ and $3T$ muscovite.

The simulations in the present study showed that in 2:1 layer silicates, such as I/S, variable fringe spacing should not automatically be used to imply that the structure possesses layers of different thickness. If a relatively large crystal containing many layers can be imaged, and a good measurement of average layer thickness can thus be obtained, values deviating appreciably from 10 Å might then be used to infer that some layers having other widths are, indeed, present. The simulations clearly showed, however, that crystals containing layers spaced at 10 Å can produce images with fringes spaced at other distances (Figure 8). The presence of fringes having more than one width therefore should not be used to infer the presence of layers of different thickness, unless electron diffraction or other data from the region support this conclusion.

Other microscopes. The above image simulations were all performed for a specific electron microscope, the Philips 420 instrument, and they should be good guides to image character for instruments having similar optical characteristics. The question arises, however, as

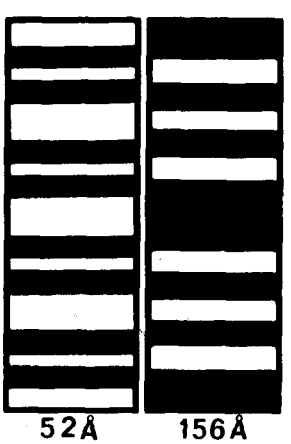


Figure 6. Comparison of images from two thicknesses of R1 ordered illite/smectite in perfect orientation, $\Delta f = +1000$ Å. (a) Simulation for crystal 10 unit cells thick (52 Å). (b) Simulation for crystal 30 unit cells thick (156 Å).

https://doi.org/10.1346/CCMN.1989.0370101 Published online by Cambridge University Press

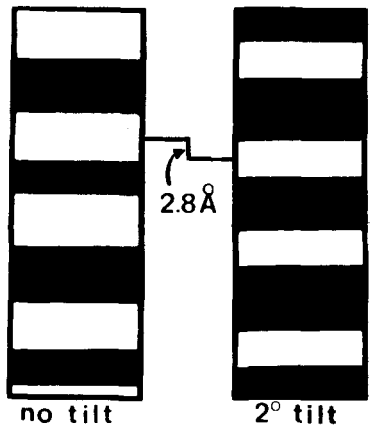


Figure 7. Comparison of tilted vs. perfectly oriented R1-ordered illite/smectite. Image of crystal tilted 3° shows positions of bright bands shifted about 3 Å from their positions in image of untilted crystal. Both images are for a Philips 420 instrument with $\Delta f = +1000$ Å; crystal thickness was 156 Å.

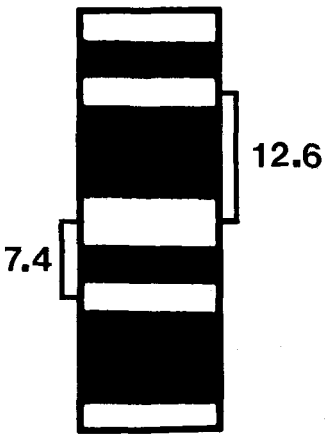


Figure 8. Simulation of R1-ordered illite/smectite for a JEOL 100C instrument operated at defocus of −135 Å. Although crystal layer thickness was exactly 10 Å, apparent variations in layer thickness exist in the image. Crystal thickness was 156 Å.

to whether investigators with access to instruments having poorer optics should be able to image ordering in I/S. To answer this question, extensive image simulations were performed for the optics of a JEOL 100C, a popular older instrument; many mineralogists have access or could obtain access to this instrument or to instruments having similar optics. As shown in the R1, one-dimensional, tilted-crystal images in Figure 9, image periodicities arising from I/S ordering occurred for conditions where focus values were +1500 Å to +2000 Å relative to the optimum (Scherzer) focus, just as they did for the Philips 420 optics. In fact, for perfectly oriented crystals, the simulations suggested that the JEOL 100C optics may actually show the periodicities due to ordering better than the Philips 420 optics, due to the way the lenses transfer specific spatial frequencies. Perfect orientation, of course, will probably be achieved over only a small fraction of the specimen area that is thin enough and crystalline enough for HRTEM observations. In any case, these simulations suggested that HRTEM studies of ordering in I/S are possible even with older instruments having relatively poor point-to-point resolution.

Image periodicities due to polytypism. Because illite and smectite interlayers can, at least theoretically, be imaged with HRTEM, it is important to ask whether other structural phenomena might produce similar effects in HRTEM images. An obvious possibility is that polytypism might lead to patterns of wide and narrow fringes similar to those produced by mixed layering in I/S. Indeed, it is well known to high-resolution microscopists who have worked with micas that $2M_1$ muscovites and biotites commonly produce one-dimensional images with two-layer periodicity (e.g., Veblen, 1983). Such images are similar, for example, to the R1-ordering simulated images at overfocus conditions shown in Figure 4. In addition, computer simulations for $2M_1$ muscovite were performed that document this phenomenon (see Figure 10). Because either mixed layering or polytypism can lead to superperiodicities in images of 2:1 phyllosilicates, an inherent ambiguity exists in the interpretation of such periodicities. This problem is addressed below. The simulations also show that polytypism can produce fringes having more than one width, even if all layers in the structure have the same thickness. This observation underscores the cautions described in the section entitled "Apparent layer thicknesses."

DISCUSSION AND CONCLUSIONS

Through the technique of HRTEM image simulation, the effects of various experimental factors on the imaging of mixed-layer 2:1 sheet silicates have been explored. These calculations have several important implications for both past and future HRTEM studies on mixed-layer I/S, as discussed below.

Conditions for observing I/S ordering

The good news is that ordering in chemically untreated I/S can be observed in one-dimensional images obtained under appropriate conditions with TEM instruments of moderate resolution (Figures 2–5 and 8). The bad news is that such ordering is observable only under certain conditions and not others. Specifically, for the underfocus conditions typically used in HRTEM studies, slight tilting of the crystal out of perfect orientation destroys any obvious modulations in image intensity related to ordering. On the other hand, for slightly tilted crystals and at overfocus values of about 1000 Å, modulations in fringe width produce distinct 20- and 40-Å periodicities for perfect R1 and R3 or-

https://doi.org/10.1346/CCMN.1989.0370101 Published online by Cambridge University Press

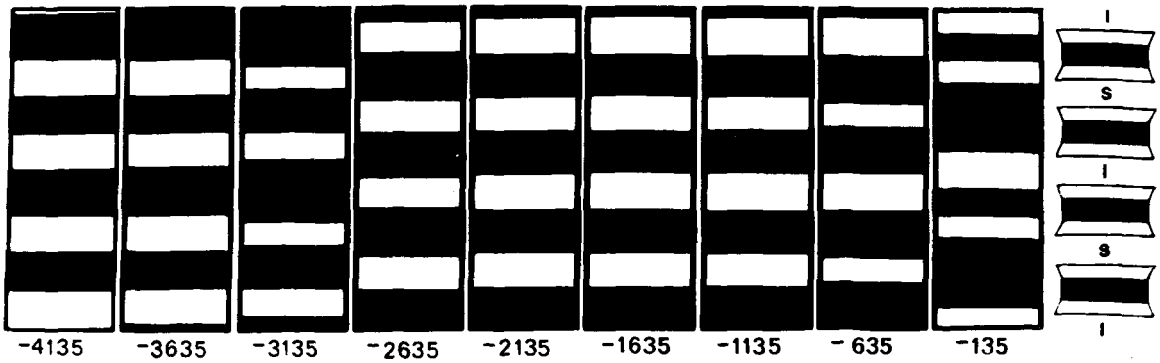


Figure 9. One-dimensional simulation of R1-ordered illite/smectite for a JEOL 100C instrument. Simulations assumed the structure to be tilted about 3°. Scherzer focus is shown in the central image. Crystal thickness was 156 Å.

dering, respectively. Under these focus conditions, however, a perfectly oriented crystal produces images in which these superperiodicities are very weak or absent. Likewise, very thin regions of a specimen may not indicate ordering, even if it is present (Figure 6).

Rapid electron beam damage of I/S precludes the careful tilting of the crystal into proper imaging orientation that is used for HRTEM studies of more stable minerals. As a result, most HRTEM images of I/S are probably obtained by achieving approximate orientation and recording images when the microscopist observes lattice fringes. In addition, experimental HRTEM studies of I/S (see Introduction for references) have shown that these materials typically occur in small packets in which the 2:1 layers have roughly the same orientation. Even within these packets, however, considerable bending of the layers exists, and such variations in orientation can be expected not only in the plane of the specimen, but also parallel to the electron beam. Therefore, most published I/S images were probably obtained from crystals that were not perfectly oriented and, indeed, having orientations that varied somewhat from region to region within any given image. Based on this assumption, the simulations described here suggest that images obtained with an overfocused microscope may have the best chance of showing the ordering of illite and smectite layers.

Given all the experimental variables and the fact that image modulations due to I/S ordering occur under only some conditions, the absence of such modulations alone should not be used to imply that a given I/S specimen is not ordered. In some specimens, discrepancies between X-ray powder diffraction (XRD) and electron microscopy studies of I/S have been noted for the same specimen. For example, Gulf Coast shales that have been shown by XRD to contain ordered mixed-layer I/S (Perry and Hower, 1970) appear to contain no ordered mixed-layer I/S when they were examined with HRTEM (e.g., Ahn and Peacor, 1986a). Possibly the apparent ordering is an artefact of the preparation procedures used for the XRD experiments; however, the TEM experiments may also have been carried out under conditions unsuitable for the observation of the mixed layering (e.g., underfocused images of crystals not in perfect orientation). Alternatively, image modulations due to I/S interlayering are relatively weak and might have been overlooked even if present. Although the present study cannot definitively resolve the discrepancy between XRD and HRTEM studies, it does constrain the experimental conditions for future studies aimed at resolving this perplexing problem.

Imaging of disordered mixed-layer I/S

The simulations presented here are for perfectly ordered I/S, specifically a perfect two-layer R1 structure and a perfect four-layer R3 structure. In nature, the exact illite : smectite ratios of 1:1 and 3:1 necessary to produce these perfectly ordered structures seldom are

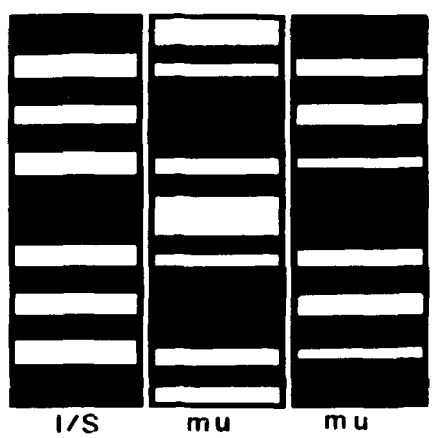


Figure 10. Comparison of images of R1-ordered illite/smectite and $2M_1$ muscovite. All three simulations were for a Philips 420 instrument and a thickness of 156 Å. Illite/smectite simulation: Perfect orientation; $\Delta f = -1000$ Å. Muscovite simulations: Near perfect orientation (structure was tilted a few tenths of a degree to allow dynamical diffraction to occur); $\Delta f = 2850$ Å, -2950 Å.

https://doi.org/10.1346/CCMN.1989.0370101 Published online by Cambridge University Press

realized, thereby requiring some disorder in the sequence of illite and smectite interlayers. Although images for such disordered I/S were not calculated, the interpretation of disordered images should pose no problem. Indeed, characterization of such disordered structures is the most important application of HRTEM. The simulations presented here show, for example, that in overfocused images of slightly tilted specimens a heavy dark fringe is present near the position of the smectite interlayers, whereas weaker dark fringes are associated with the illite interlayers. Therefore, the exact sequence of illite and smectite layers can probably be determined from images of this sort, whether from ordered or disordered material. Work in progress in this laboratory suggests that this result from the simulations is consistent with experiment.

Correspondence between image and structure

As discussed above, the simulations described here show that the positions of light and dark fringes relative to the 2:1 layers and interlayers of I/S depend on focus and crystal thickness. In addition, for a given focus and thickness, the fringes change in their details and thicknesses and shift relative to the structure if the crystal is tilted out of perfect orientation. The dark fringes in an image are not the 2:1 layers; rather, they are simply "lattice fringes," and their exact positions relative to the actual crystal structure are a complicated function of many electron optical parameters. Only in the light of detailed image simulations and with complete knowledge of the imaging conditions, including the exact crystal orientation, can an exact correspondence be made between details in a HRTEM image and specific structural features in the crystal.

Distinguishing between I/S ordering and polytypism

As has been shown, polytypism in 2:1 layer silicates can produce contrast in HRTEM images that might be confused with that from mixed layering in I/S. For example, an image of R1 I/S might be very similar to an image of a $2M_1$ mica. Given this ambiguity, it is important to ask whether there is any way to distinguish between contrast variations due to I/S mixed layering and those due to polytypism.

Given the difficulties in imaging I/S with HRTEM and in thoroughly characterizing the imaging conditions, no simple way appears to exist, on the basis of electron optics, to attribute contrast modulations in any specific image to mixed layering vs. polytypism. For many materials, however, polytypism can be ruled out on the basis of other information (e.g., XRD experiments).

For other materials, geological constraints on the occurrence and polytypic state of I/S may provide a reasonable basis for interpretation. For example, in their study on the shales and slates from Lehigh Gap, Pennsylvania, Lee *et al.* (1986) showed that (1) complete stacking disorder exists in illite and I/S in the shales; (2) with progressive diagenesis and metamorphism, the stacking-disordered clays were transformed to $1M_d$ muscovite; and (3) only after this transformation to mica did the 2:1 layer silicate become polytypically ordered. Thus, in many rock types, I/S may always be relatively disordered polytypically and may not coexist with polytypically ordered 2:1 structures. Furthermore, even if detrital $2M_1$ muscovite or biotite occurs with I/S, the I/S and mica should be distinguishable with analytical electron microscopy. Thus, for many types of studies, the potential ambiguity in interpretation of superperiodicities in HRTEM images from 2:1 layer silicates may be eliminated by other forms of evidence.

ACKNOWLEDGMENTS

This work has benefited enormously from discussions with numerous individuals, including R. C. Reynolds, K. J. T. Livi, M. DiStefano, J. F. Banfield, and P. J. Heaney. We thank M. A. O'Keefe not only for insightful discussions over the years on image simulation, but also for providing us with the SHRLI software. Helpful comments on the original manuscript were provided by I. D. R. Mackinnon, D. R. Peacor, and F. A. Mumpton. We gratefully acknowledge financial support for this research by Conoco, Inc., and NSF grant EAR86-09277. The computational facility used for this project was acquired with partial support from NSF grant EAR84-19252.

APPENDIX

All image simulations were calculated using atomic positions derived from the dioctahedral mica structure reported by Richardson and Richardson (1982). The composition and stacking sequence of the mica, however, were altered to obtain the structures needed for the various simulations.

Although illite is generally believed to have a layer charge of 0.75, recent work by Środoń and coworkers suggests that illite may be a mechanical mixture of two illites having layer charges of 0.55 and 1.00 (Środoń and Eberl, 1984). All simulations in this work, however, assumed the illite layers to have a uniform layer charge of 0.75. Though "ideal" smectite is commonly assumed to have a layer charge of 0.33, natural smectites exhibit a range of layer charges from 0.2 to 0.6 (Brindley, 1981). The minimum layer charge for smectite, 0.2, was used in these simulations, thereby maximizing the compositional difference between smectite and illite. The smectite mineral represented in these calculations was beidellite; in other words, the source of the layer charge was the tetrahedral layer, which was compensated by the interlayer substitution of vacancies for K^+.

All simulated illite/smectite images assumed a $1M$ stacking sequence for the sheets. The structure of an individual layer of the $2M_1$ structure (space group $C2/c$) of Richardson and Richardson (1982) was transformed into the standard $1M$ unit cell (space group $C2/m$). The unit-cell transformation matrix, T, was the following:

https://doi.org/10.1346/CCMN.1989.0370101 Published online by Cambridge University Press

Table A-1. Fractional coordinates of atom positions used in simulations.

Atom		R & R (1982)[1]	x'_{new}[2]	x_{input}[3]
K	x	0.0000	0.0000	0
	y	0.0992	0.0000	0
	z	0.2500	0.0000	0
Si(A)	x	0.4510		
	y	0.2587		
	z	0.1355		
Si(B)	x	0.0354	0.5819	0.5819
	y	0.4298	0.1703	0.1703
	z	0.3646	0.2292	0.2292
Al(Oct.)	x	0.2506	0.4997	0
	y	0.0838	0.3328	0.8328
	z	0.0002	0.5004	1/2
O(A)	x	0.3872	0.3305	0.8305
	y	0.2525	0.7220	0.2220
	z	0.0543	0.1630	0.1630
O(B)	x	0.0366	0.5014	0.5014
	y	0.4431	1.0000	0
	z	0.4459	0.1848	0.1848
O(C)	x	0.4178	0.6507	0.6507
	y	0.0931	0.1925	0.1925
	z	0.1685	0.3918	0.3918
O(D)	x	0.2475		
	y	0.3712		
	z	0.1685		
O(E)	x	0.2509		
	y	0.3132		
	z	0.3424		
OH	x	0.0422	0.0842	0.0842
	y	0.0622	0.9999	0
	z	0.4492	0.3984	0.3984

[1] Coordinates for $2M_1$ muscovite from Richardson and Richardson (1982).

[2] R & R coordinates transformed to $1M$ setting.

[3] Atom positions used in the simulations.

$$T = \begin{vmatrix} 0.5 & 0.5 & 0.0 \\ -1.5 & 0.5 & 0.0 \\ 0.0 & -0.1984 & 0.5 \end{vmatrix}. \quad (1)$$

Transformed atom positions were obtained from the relationship

$$x_{new} = C \cdot x_{old}, \quad (2)$$

where x_{new} and x_{old} are matrices representing the new and old fractional coordinates of the atoms, and C is the matrix

$$C = (T^T)^{-1}, \quad (3)$$

or simply the inverse of the transpose of the unit-cell transformation matrix. The origin of the unit cell was then shifted such that it corresponded to the position of a potassium atom. Specifically,

$$x'_{new} = x_{new} - 0.2976 \quad (4a)$$

$$y'_{new} = y_{new} - 0.0992 \quad (4b)$$

$$z'_{new} = z_{new} - 0.5. \quad (4c)$$

Finally, the positions of some atoms were shifted slightly to lie on the $C2/m$ symmetry operators. Individual layers were stacked along the c-axis of the $1M$ setting to obtain the various structures. Table A-1 gives the old fractional coordinates from Richardson and Richardson (1982), the new fractional coordinates calculated from Eq. (4), and the final fractional coordinates used in the calculations for one layer.

Simulations for $2M_1$ muscovite were calculated using the structure of Richardson and Richardson (1982). Aluminum was assumed to occupy one quarter of the tetrahedral sites, and potassium was assumed to occupy all of the interlayer sites.

REFERENCES

Ahn, J. H. and Peacor, D. R. (1985) Transmission electron microscopic study of diagenetic chlorite in Gulf Coast argillaceous sediments: *Clays & Clay Minerals* **33,** 228–236.

Ahn, J. H. and Peacor, D. R. (1986a) Transmission and analytical electron microscopy of the smectite-to-illite transition: *Clays & Clay Minerals* **34,** 165–179.

Ahn, J. H. and Peacor, D. R. (1986b) Transmission electron microscope data for rectorite: Implications for the origin and structure of "fundamental particles": *Clays & Clay Minerals* **34,** 180–186.

Amouric, M., Mercuriot, G., and Baronnet, A. (1981) On computed and observed HRTEM images of perfect mica polytypes: *Bull. Mineral.* **104,** 298–313.

Bell, T. E. (1986) Microstructure in mixed-layer illite/smectite and its relationship to the reaction of smectite to illite: *Clays & Clay Minerals* **34,** 146–154.

Brindley, G. W. (1981) Structures and chemical compositions of clay: in *Clays and the Resource Geologist,* F. J. Longstaffe, ed., Short Course Handbook 7, Mineral. Assoc. Canada, Toronto, 1–21.

Cowley, J. and Moodie, A. F. (1957) The scattering of electrons by atoms and crystals. I. A new theoretical approach: *Acta Crystallogr.* **10,** 609–619.

Hansen, P. L. and Lindgreen, H. (1987) Structural investigations of mixed-layer smectite-illite clay minerals from North Sea oil source rocks: in *Proc. Conf. Electron Micro. Soc. Amer.,* Baltimore, Maryland, *1987,* G. W. Bailey, ed., San Francisco Press, San Francisco, 374–375.

Iijima, S. and Buseck, P. R. (1978) Experimental study of disordered mica structures by high-resolution electron microscopy: *Acta Crystallogr.* **A34,** 709–719.

Klimentidis, R. E. and Mackinnon, I. D. R. (1986) High-resolution imaging of ordered mixed-layer clays: *Clays & Clay Minerals* **34,** 155–164.

Lee, J. H., Ahn, J. H., and Peacor, D. R. (1985) Textures in layered silicates: Progressive changes through diagenesis and low-temperature metamorphism: *J. Sed. Petrol.* **55,** 532–540.

Lee, J. H., Peacor, D. R., Lewis, D. D., and Wintsch, R. P. (1986) Evidence for syntectonic crystallization for the mudstone to slate transition at Lehigh Gap, Pennsylvania: *J. Struct. Geol.* **8,** 767–780.

McKee, T. R. and Buseck, P. R. (1978) HRTEM observations of stacking and ordered interstratification in rectorite: in *Electron Microscopy 1978, Vol. 1,* J. M. Sturgess, ed., Microscopical Society of Canada, Toronto, 272–273.

O'Keefe, M. A. (1984) Electron image simulation: A complementary processing technique: in *Electron Optical Systems,* SEM Inc., AMF O'Hare, Chicago, 209–220.

O'Keefe, M. A., Buseck, P. R., and Iijima, S. (1978) Computed crystal structure images for high resolution electron microscopy: *Nature* **274,** 322–324.

Perry, E. and Hower, J. (1970) Burial diagenesis in Gulf Coast pelitic sediments: *Clays & Clay Minerals* **18,** 165–177.

Richardson, S. M. and Richardson, J. W., Jr. (1982) Crystal structure of a pink muscovite from Archer's Post, Kenya:

https://doi.org/10.1346/CCMN.1989.0370101 Published online by Cambridge University Press

Implications for reverse pleochroism in dioctahedral micas: *Amer. Mineral.* **67,** 69–75.

Self, P. G. and O'Keefe, M. A. (1988) Calculation of diffraction patterns and images for fast electrons: in *High Resolution Transmission Electron Microscopy,* P. R. Buseck, J. M. Cowley, and L. Eyring, eds., Oxford University Press (in press).

Spence, J. C. H. (1981) *Experimental High-Resolution Electron Microscopy:* Clarendon Press, Oxford, England, 370 pp.

Spinnler, G. E., Self, P. G., Iijima, S., and Buseck, P. R. (1984) Stacking disorder in clinochlore chlorite: *Amer. Mineral.* **69,** 252–263.

Środoń, J. and Eberl, D. D. (1984) Illite: in *Micas, Reviews in Mineralogy, Vol. 13,* S. W. Bailey, ed., Mineral. Soc. Amer., Washington, D.C., 495–544.

Veblen, D. R. (1983) Microstructures and mixed layering in intergrown wonesite, chlorite, talc, biotite, and kaolinite: *Amer. Mineral.* **68,** 566–580.

Veblen, D. R. (1985a) High-resolution transmission electron microscopy: in *Applications of Electron Microscopy in the Earth Sciences, Short Course Handbook, 1985,* J. C. White, ed., Mineral. Assoc. Canada, Toronto, Canada, 63–90.

Veblen, D. R. (1985b) Direct TEM imaging of complex structures and defects in silicates: *Ann. Rev. Earth Planet. Sci.* **13,** 119–146.

Veblen, D. R. (1989) Transmission electron microscopy: Scattering processes, conventional TEM, and high-resolution imaging: in *Electron Microscopy and Microprobe Techniques in Clay Analysis, CMS Workshop Lectures,* I. D. R. Mackinnon and F. A. Mumpton, eds., The Clay Mineral Society, Bloomington, Indiana (in press).

(Received 11 March 1988; accepted 6 August 1988; Ms. 1772)

https://doi.org/10.1346/CCMN.1989.0370101 Published online by Cambridge University Press